ChemPubSoc Europe

DOI: 10.1002/chem.201600917

CHEMISTRY
A European Journal
Communication

Fused Heterocycles

Aromatic Fused [30] Heteroannulenes with NIR Absorption and NIR Emission: Synthesis, Characterization, and Excited-State Dynamics

Abhijit Mallick,[a] Juwon Oh,[b] Dongho Kim,*[b] and Harapriya Rath*[a]

Dedicated to Professor Tavarekere K Chandrashekar

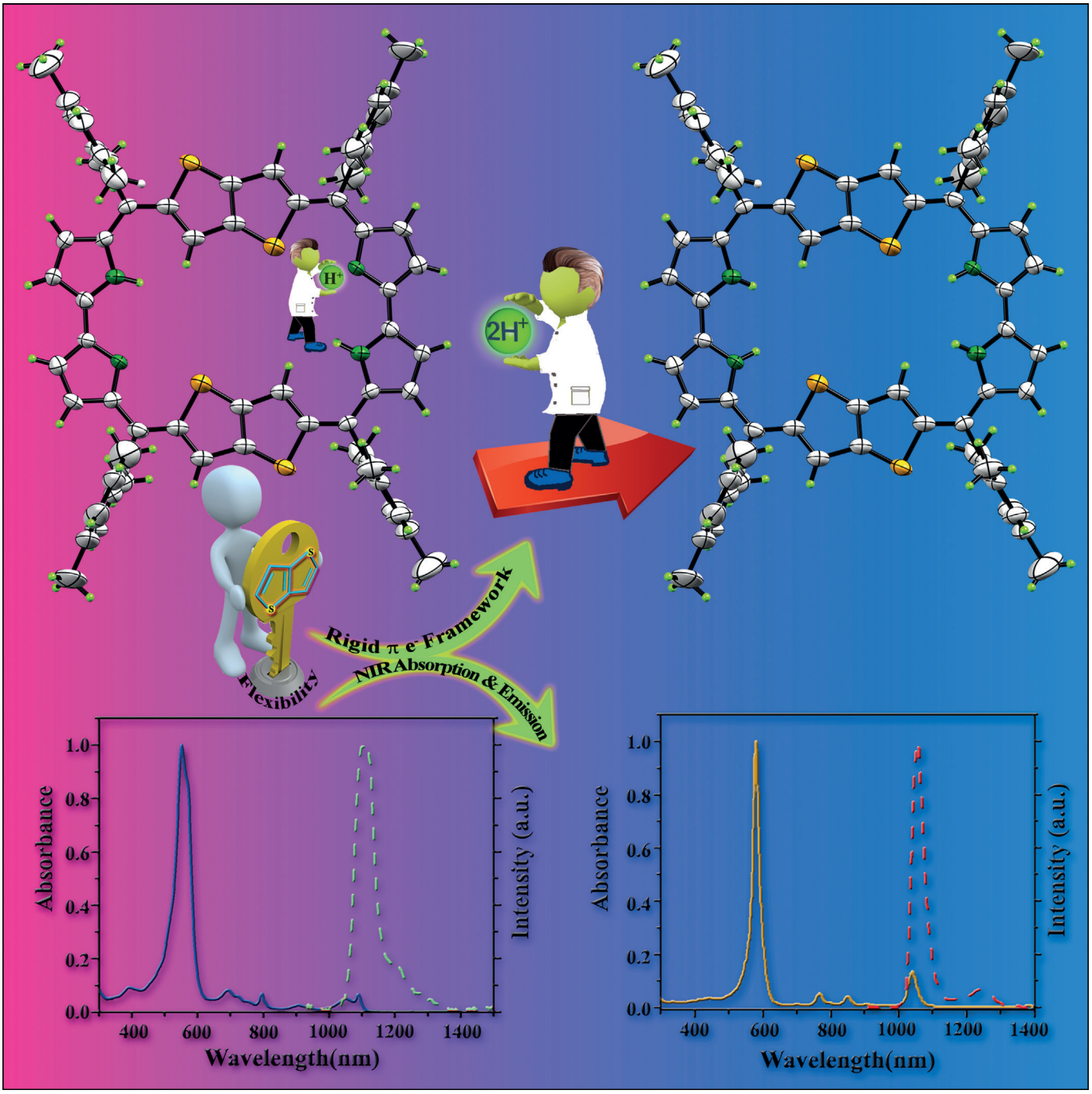

Abstract: Two hitherto unknown planar aromatic [30] fused heterocyclic macrocycles (1.1.0.1.1.0), with NIR absorption in free-base form and protonation-induced enhanced NIR emission, have been synthesized from easy to make precursors. The induced correspondence of fusion on the macrocyclic structure, electronic absorption, and emission spectra have been highlighted.

Recent developments in many different fields of modern science and medicine, such as molecular biology, material science, drug discovery, and tissue diagnostics have fueled the design of new chromophores that can absorb and/or emit within the red or near infrared (NIR) region of the spectrum.[1] In this context, expanded porphyrins have earned increasing interest as being one of the more versatile heterocyclic skeleton chromophores.[2] These macrocycles possess electrical properties and outstanding optical properties that make them perfect building blocks for incorporation into multifunctional materials. Under these fascinating attributes of expanded porphyrins, their aromatic nature plays a crucial role since aromaticity controls stability, structure, and reactivity of expanded porphyrins. However, the conformational flexibility and complexity in the assessment of diatropicity becomes more perceptible for larger expanded porphyrins.[3] In this context, controlled modifications of the basic framework of expanded porphyrins results in systematic variation of the optical properties, making them efficient NIR dyes in specific instances.[4] Effective construction of aromatic macrocycles with extended conjugation requires a subtle balance of appropriate geometric conformation fused to electronic stability derived from increased delocalization.[5]

With the insight from our recent observation,[4a] where fused ring expansion of the pyrrole moieties at the β positions and fused thiophene moieties resulted in NIR absorption, efforts were directed towards the synthesis of higher analogues (Scheme 1) with free pyrrole moieties and fused thiophene moieties in order for the constructs to be rigidly planar and fully conjugated across the entirety of the porphyrinoid backbone. Based on our target macrocycles, the fused thieno [3, 2-*b*] thiophene **1** has been synthesized following a literature report.[6] Because the steric factor of the *meso*-aryl substituents play a decisive role in cyclizing the precursors,[7] the desired precursors **4** and **5** were synthesized in quantitative yields

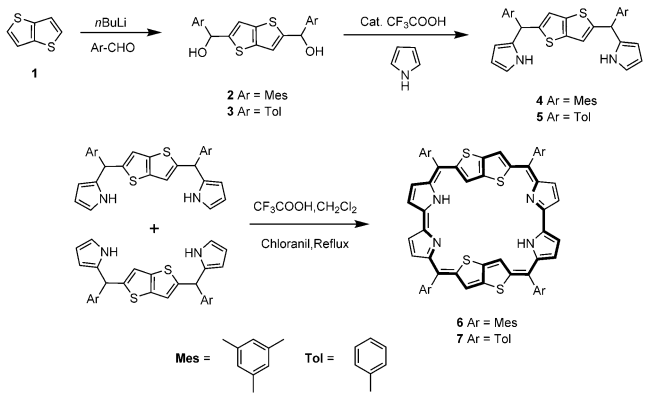

Scheme 1. Synthesis of macrocycles **6** and **7**.

from **2** and **3** (Scheme 1). Rational synthesis of macrocycles **6** and **7** entails self-coupling of **4** and **5** using trifluoroacetic acid as the catalyst and chloranil as oxidant.[8] One equivalent of trifluoroacetic acid gave the best yields for macrocycles **6** and **7**. Formation of the macrocycles at moderate concentration of trifluoroacetic acid indicates the α–α self-coupling of precursors **4** and **5** with the formation of two direct pyrrole–pyrrole links to form an intermediate porphyrinogen, which on subsequent oxidation with chloranil yielded the desired [30]π conjugated macrocycles **6** or **7**. Column chromatographic separation over basic alumina, followed by repeated silica gel (200–400 mesh) chromatographic separation, yielded the macrocycles **6** and **7** in 5 and 6% yields, respectively, as dark green solid. Acid concentration above one equivalent of trifluoroacetic acid led to acidolysis of the precursors **4** and **5** and yielded [22] heterocyclic macrocycles.[4a]

The new macrocycles have been characterized via spectroscopic and single-crystal X-ray diffraction analyses. Macrocycle **6** shows a parent ion peak at *m/z* 1058.641, whereas macrocycle **7** shows a parent ion peak at 948.515 under positive ionization conditions in MALDI-TOF mass spectrometry, thus confirming the proposed composition for the macrocycles. The absorption spectra of **6** and **7** showed typical characteristics of aromatic porphyrinoids, with the intense B-like bands at 550 nm and weak Q-like bands in the range of 692–1088 nm (Figure 1).[9] The NIR emission at 1089 and 1068 nm for **6** and **7**, respectively, supports their aromatic character.[10a] Compared to the weak and broad absorption and non-emissive behavior of dithiahexaphyrin,[11] the spectral features of **6** and **7** are ascribed to the impact of fused thienothiophene moieties, which

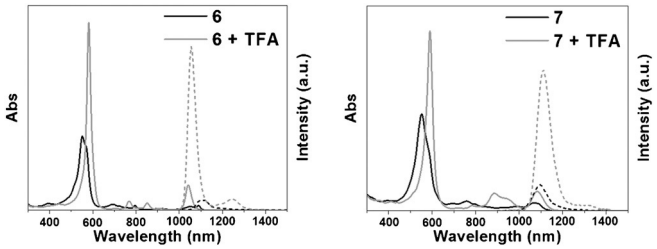

Figure 1. UV/Vis Spectra and Emission Spectra of **6** (left) and **7** (right).

[a] *A. Mallick, Prof. Dr. H. Rath*
Department of Inorganic Chemistry
Indian Association for the Cultivation of Science
2A/2B Raja S. C. Mullick Road, Jadavpur, Kolkata 700 032 (India)
Fax: (+91) 33-24732805
E-mail: ichr@iacs.res.in

[b] *J. Oh, Prof. Dr. D. Kim*
Department of Chemistry
Yonsei University, Seodaemun-gu, Seoul 120-749 (Korea)
E-mail: dongho@yonsei.ac.kr

Supporting information for this article, which includes full experimental details, is available on the WWW under http://dx.doi.org/10.1002/chem.201600917.

induce relatively rigid and planar structures with a fully π-conjugated system, leading to the NIR absorption and emission. Protonation of **6** and **7** results in further redshifts of B- and Q-like bands with an increase of extinction coefficient of the Soret maxima. Furthermore, their redshifted NIR emission was enhanced almost 16- and 7 times, respectively, compared to that of free base **6** and **7** with the reduced Stokes shifts ($174 \rightarrow 118\ cm^{-1}$ for **6** and $222 \rightarrow 175\ cm^{-1}$ for **7**). These features indicate that protonation provides the structural rigidity and induces smoother π-conjugation by cut-off of intramolecular hydrogen-bonding interactions between pyrrole moieties.[10] Here, compared to protonated **7**, more enhanced NIR emission and smaller Stokes shift of protonated **6** suggest that this has a more rigid structure due to steric effects caused by the *meso*-mesityl substituents.

The ^{1}H NMR spectral patterns provide ample evidence for the macrocyclic aromaticity through a [30]π electronic delocalization motif both in free base as well as in protonated form. Due to the characteristic diatropic ring current effect, the protons inside the macrocycle resonate in the up-field region and the protons on the periphery resonate in the deshielded region. Figure 2 depicts representative ^{1}H NMR spectra of free base **6** and protonated **6**. At 298 K, the free-base form of **6** exhibits two signals in the shielded region at −2.43 and at −6.15 ppm. The signal at −2.43 ppm has been unambiguously assigned to the NH peak after a D_2O exchange experiment (see Figure S22 in the Supporting Information). The scalar coupling between the signal at −2.43 ppm with the broad signals at 11.06 and 10.08 ppm in 2D COSY spectra (Figure S21A in the Supporting Information) confirms the later signals as β-CHs of pyrrolic rings. Furthermore, the signal at −2.43 ppm exhibits dipolar coupling with the signal at −6.15 ppm in 2D ROESY spectra (Figure S21B in the Supporting Information) confirming the latter signal as inner β-CH of thienothiophene ring. In the deshielded zone, the broad signal at 11.62 ppm correlating with the signal at 2.17 ppm in 2D ROESY spectra (Figure S21B in the Supporting Information) clearly indicates the former signal as outer β-CH of thienothiophene ring. Hence, the broad signals at 10.14 and 10.94 ppm that exhibit scalar coupling among themselves in 2D COSY spectra (Figure S21A in the Supporting Information) have been unequivocally assigned to outer β-CHs of pyrrolenic rings. With these observations, the free base **6** can be gauged as [30] π electronic macrocycle having no pyrrole ring inversion. The calculated $\Delta\delta$ value from chemical shift is found to be 17.77 ppm, thus suggesting aromaticity in this macrocycle.[12] The ^{1}H NMR signals of the free-base form of **6** are broadened beyond interpretation as we carried out low temperature NMR studies (Figure S20 in the Supporting Information), suggesting the dynamic behavior of the macrocycle. We cannot exclude the presence of minor tautomer **6B** as a consequence of the failure to arrive at well-resolved peaks.[8a] This points to the presence of **6A** as the only tautomer or alternatively to a fast equilibrium between **6A** and **6B** strongly shifted towards **6A** (Scheme S2 in the Supporting Information). In the next step, we tried to study the impact of protonation on the aromaticity and conformational change(s) in the macrocycle. Upon protonation, partially resolved spectra could be obtained due to aggregation but careful addition of CD_3OD (20 μL) gave a well-resolved spectra with the missing signal for NH proton (Figure S25 in the Supporting Information), which could be resolved only at low temperature (Figure S26 in the Supporting Information). At 253 K, the NMR spectrum of completely protonated **6** (Figure 2) displayed the characteristic features of an aromatic macrocycle in solution state. The ^{1}H NMR spectrum of protonated **6** at 253 K showed two distinctly different broad signals for NH protons at −5.64 and −5.36 ppm, confirmed by D_2O exchange spectra (Figure S29 in the Supporting Information). In the deshielded region, there are two closely placed doublets at 11.63 and 11.61 ppm and another set of doublets at 10.70 and 10.76 ppm. As the second most conceptual step of analysis of NMR spectra, 2D COSY and ROESY spectra were recorded. In the 2D COSY spectra (Figure S27 in the Supporting Information), the two sets of doublets at 11.61 and 11.63 ppm, corresponding to one proton each, show correlation with doublets at 10.76 and 10.70 ppm, respectively. Moreover, all four sets of

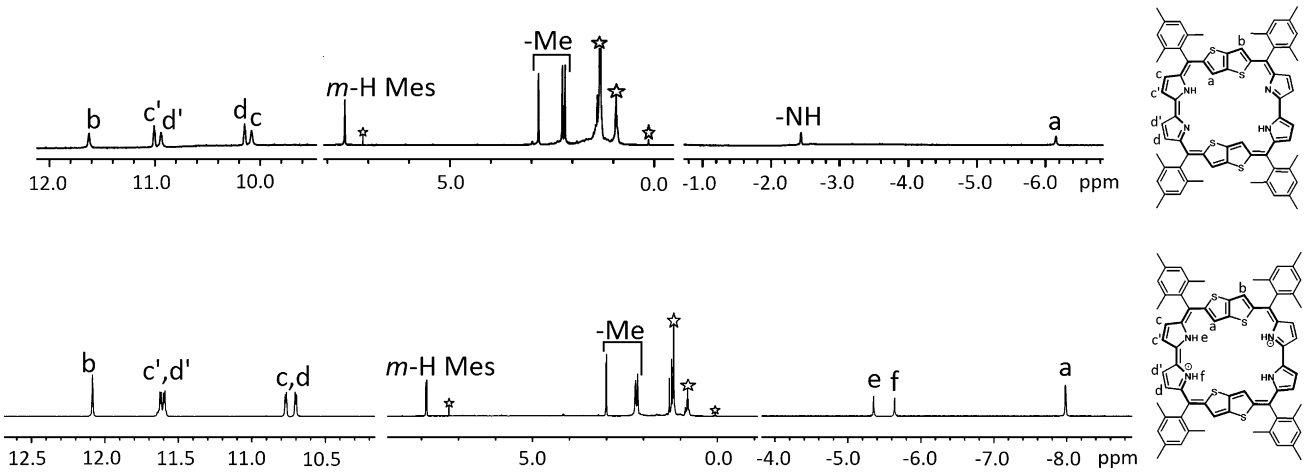

Figure 2. ^{1}H NMR spectra of free-base **6** (top) in $CDCl_3$ at 298 K and protonated **6** (bottom) in $CF_3COOH/CDCl_3$ at 253 K (* indicates residual solvent peak or solvent impurity).

doublets exhibit scalar coupling with the NH signals at −5.64 and −5.36 ppm that was informative enough for correct assignment of peaks as pyrrolic β-CHs. Furthermore, this interpretation is reinforced by the observation of two sets of dipolar couplings between the signal at 10.76 ppm with the signal at 2.02 ppm and between signals at 10.70 ppm with that at 2.21 ppm in 2D ROESY spectra (Figure S28 in the Supporting Information). The singlet at 12.08 ppm, which doesn't exhibit scalar coupling with any other signal(s) in 2D COSY spectra but exhibit dipolar coupling with the signal at 2.02 ppm in ROESY spectra (Figure S28 in the Supporting Information), has been unequivocally assigned to the outer β-CH of the thienothiophene. The sharp singlet at −7.98 ppm exhibits dipolar coupling with the NH signal at −5.34 ppm in 2D ROESY spectra, confirming this to be the inner β-CH of the thienothiophene moiety. With these observations, protonated **6** can be ascribed as [30] π electronic macrocycle having no pyrrole ring inversion similar to its free-base form. The calculated $\Delta\delta$ value from chemical shift is found to be 20.07 ppm, thus suggesting aromaticity in this macrocycle.[12] An enhanced aromaticity in the protonated form of **6** compared to the free-base form of **6** is in accordance with the absorption and emission spectral changes upon protonation, indicating that protonation induces a more rigid structure with enhanced π-electron delocalization. For macrocycle **7**, due to insolubility, it was difficult to arrive at an assignable spectrum in the free-base form. However, upon protonation using 10% CF_3COOH/CD_2Cl_2, at 243 K, we could arrive at well-assigned spectra (Figure S33 in the Supporting Information). There are three signals at −3.74, −3.39, and −3.06 ppm. The signals at −3.06 and −3.39 ppm have been assigned to NHs of the pyrrole rings after D_2O exchange experiments (Figure S36 in the Supporting Information).

Unfortunately, no scalar coupling between these two signals with signals in the deshielded region were observed in 2D COSY spectra. However, the dipolar coupling between the signals at −3.39 ppm with −3.74 ppm (Figure S35 in the Supporting Information) convinced us to assign the later signal as inner β-CH of thienothiophene ring. In the 2D COSY spectra (Figure S34 in the Supporting Information), the correlation between signals at 2.37 ppm with broad signals at 8.5–8.12 ppm and 2.88 ppm with signals at 7.73 ppm clearly indicates that the signals in the aromatic zone correspond to *meso*-tolyl CHs. Hence, the signals in the deshielded region at 10.38 ppm, which exhibit no correlation with any signal(s) in 2D COSY spectra, have been unambiguously assigned to the outer β-CH of the thienothiophene ring. The remaining broad signals from 9.7 to 10.80 ppm, which exhibit scalar couplings among themselves, unequivocally belong to the outer β-CHs of pyrrole rings (Figure S34 in the Supporting Information). The calculated $\Delta\delta$ value (difference in chemical shift between inner NH/CH and outer NH/CH protons in ^{1}H NMR spectrum) from chemical shift is found to be 14.54 ppm, thus suggesting aromaticity in this macrocycle. The smaller $\Delta\delta$ value in the macrocycle **7** compared to **6** is due to the fact that *meso*-mesityl substituents impart more structural rigidity to the macrocycle **6** compared to more flexible *meso*-tolyl in **7**, as discussed in the absorption and emission spectra.

Redox properties of these new macrocycles have been studied with the help of cyclic voltammetry and differential pulse voltammetry in dichloromethane using 0.1 M tetrabutyl ammonium hexafluorophosphate as a supporting electrolyte. Macrocycle **6** exhibits one irreversible oxidation peak at 0.30 V, followed by two reversible oxidation peaks at 0.55 and 0.78 V, and two reversible reduction peaks at −0.95 and −1.24 V with HOMO–LUMO gap estimated at 1.25 V (Figure S38 in the Supporting Information). This value is apparently much lower than that of *meso*-tetraphenyl porphyrin (2.26 V)[13] and [26] tetrathia rubyrin.[3a] This phenomenon may be due to fusion of thiophene rings into the core of the macrocycle, leading to rearrangement of HOMO–LUMO, which is an offshoot of such core modifications that leads to decrease in Δ_{redox} value. For macrocycle **7**, electrochemical studies could not be carried out due to very low solubility in any organic solvent.

To gain further insights into the conformation of **6** and **7**, solid-state X-ray crystallographic analysis and density functional theory (DFT) calculations have been performed. For macrocycles **6** and **7**, failure to obtain a good single crystal suitable for X-ray diffraction in the free-base form forced us to resort to geometry optimization based on ^{1}H NMR spectra to arrive at the proposed structure of the macrocycles on DFT-formalism.[14] The optimized structures of **6** and **7** (Figure S39 in the Supporting Information) showed planar geometries with mean plane deviation (MPD) values of 0.057 and 0.144 Å, respectively. On the other hand, single crystals suitable for X-ray diffraction were obtained by slow diffusion of hexane into a TFA/dichloromethane solution of **6**. Macrocycle **6**, upon protonation, turned out to be of flat geometry (Figure 3).[15] The four *meso*-

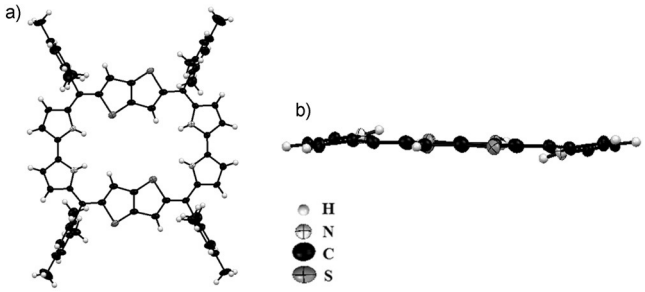

Figure 3. X-ray crystal structure of protonated **6**. Top view (a) and side view (b).

carbons lie in the macrocyclic plane. The dihedral angle for the protonated pyrrole ring is 16.70° and for neutral pyrrole ring is 11.71° above and below the mean plane containing four *meso* carbons. Based on the crystal structure of protonated **6**, we obtained optimized structures of protonated **6** and **7** (Figure S40 in the Supporting Information). Compared to freebase **6** and **7**, the protonated **6** and **7** exhibited more distorted structures due to the steric repulsion between pyrrolic protons and inner β-CH protons of thienothiophene moiety (MPD values of 0.228 and 0.304 Å for protonated **6** and **7**, respectively). It was noted that the dihedral angles of *meso*-mesityl substituents 76.5°~89.1° are larger than those of *meso*-tolyl substituents 51.3°~

64.4°, reflecting the larger steric effect of mesityl substituents on the macrocycle along with their MPD values.

To gain deeper insights into the aromaticity of **6** and **7**, we conducted nucleus-independent chemical shift (NICS)[16] calculations. In line with the ^{1}H NMR spectra of **6** and **7**, their NICS values at the center of the macrocycles were estimated to be −14.4 and −14.3 ppm (Figures S41 and S42 in the Supporting Information), indicating aromatic character. This aromatic character was clearly illustrated by Anisotropy of the Induced Current Density (ACID) plots,[17] where the distinct clockwise ring currents of free-base and protonated **6** and **7** visualized their aromatic nature (Figures S43 and S44 in the Supporting Information). Furthermore, the estimated Harmonic Oscillator Model of Aromaticity (HOMA)[18] values (Figures S41 and S42 in the Supporting Information) and degenerate frontier molecular orbital (FMOs) with energy level diagrams (Figures S45 and S46 in the Supporting Information) are well matched with their aromatic nature.

The excited-state dynamics of free-base and protonated **6** and **7** were investigated by femtosecond transient absorption (TA) measurements. The TA spectra of freebase **6** and **7** exhibited intense ground-state bleaching (GSB) signals, corresponding to their absorption spectral features, with relatively weak excited-state absorption on both sides of the GSB signals (Figure 4). The decays of these TA spectra were fitted with two time constants; one is in hundreds ps time scales and another is longer than 10 ns, where the shorter time constants arise from intersystem crossing process and the deactivation of lowest singlet excited state. The longer time constants are assigned as the lifetime of triplet state. These TA spectral features are similar to those of typical aromatic expanded porphyrins, being well-matched with the aromatic nature of **6** and **7**.[10a] The protonation of **6** and **7** caused the change of their excited-state dynamics. In their TA spectra, the GSB signals became redshifted, sharpened, and prominently intensified (Figure S47 in the Supporting Information). Furthermore, the excited-state lifetime of the lowest singlet states were increased to 370 and 200 ps for protonated **6** and **7**, respectively. Along with the enhanced NIR absorption and emission, as well as ^{1}H NMR results, these changes in the excited-state dynamics are attributable to the more rigid structure and enhanced aromaticity upon protonation.[10] It was noted that the excited-state lifetime of protonated **6** is longer than that of protonated **7**, indicating that the steric effect of *meso*-mesityl substituents affords more structural rigidity to the macrocycle.

In conclusion, we have synthesized two new fused heterocyclic macrocycles through easily available precursors, which will allow further exploitation of their rich chemistry in terms of their coordination behavior towards transition metals and their use as catalysts for organic transformation. Moreover, as electronically attractive as these macrocycles are due to NIR absorption and NIR emission, they may be potent candidates for biomedical applications. Such thriving research activity is currently underway in our laboratory.

Acknowledgements

The work at IACS, Kolkata was supported by DST-SERB (SR/S1/IC-37/2012), CSIR (02(0120)/13/EMR-II), New Delhi, India and DST-SERB Ramanujan Fellowship (SR/S2/RJN-93/2011), India. A.M. thanks CSIR for senior research fellowship. The work at Yonsei University was supported by the Global Research Laboratory Program (2013K1A1A2A02050183) funded by the Ministry of Science, ICT & Future, Korea. The quantum calculations were performed using the supercomputing resources of the Korea Institute of Science and Technology Information (KISTI). We are indebted to the Single Crystal X-Ray Diffractometer facility in IISER, Pune, India. Our sincere thanks to Dr. R. Natarajan, IICB, Kolkata for final refinement of crystal data.

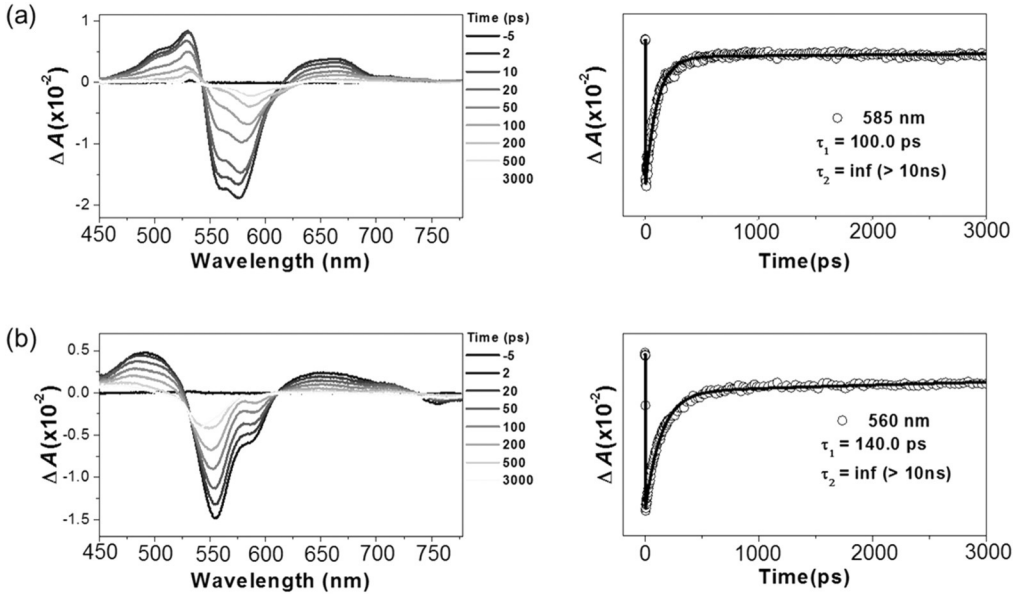

Figure 4. The femtosecond transient absorption (fs-TA) spectra (left) and decay profiles (right) of free-base (a) **6** and (b) **7** with photoexcitation at 530 nm.

Keywords: aromaticity · fused heterocycles · heteroannulenes · NIR absorption · NIR emission

[1] a) M. Wainwright, *Color. Technol.* **2010**, *126*, 115; b) M. Pawlicki, H. A. Collins, R. G. Denning, H. L. Anderson, *Angew. Chem. Int. Ed.* **2009**, *48*, 3244; *Angew. Chem.* **2009**, *121*, 3292; c) P. A. Bouit, D. Rauh, S. Neugenbauer, J. L. Delgado, E. D. Piazza, S. Rigaut, O. Maury, C. Andraud, V. Dyakonov, N. Martin, *Org. Lett.* **2009**, *11*, 4806.

[2] a) J. L. Sessler, S. J. Weghorn, *Expanded, Contracted and Isomeric Porphyrins*, Pergamon, New York, **1997**, *15*, 429; b) S. Saito, A. Osuka, *Angew. Chem. Int. Ed.* **2011**, *50*, 4342; *Angew. Chem.* **2011**, *123*, 4432.

[3] a) T. K. Chandrashekar, S. Venkataraman, *Acc. Chem. Res.* **2003**, *36*, 676; b) M. Stępień, N. Sprutta, L. Latos-Grażyński, *Angew. Chem. Int. Ed.* **2011**, *50*, 4288; *Angew. Chem.* **2011**, *123*, 4376; c) A. Osuka, S. Saito, *Chem. Commun.* **2011**, *47*, 4330.

[4] a) H. Rath, A. Mallick, T. Ghosh, A. Kalita, *Chem. Commun.* **2014**, *50*, 9094; b) J. Y. Shin, H. Furuta, A. Osuka, *Angew. Chem. Int. Ed.* **2001**, *40*, 619; *Angew. Chem.* **2001**, *113*, 639; c) T. D. Lash, *J. Porphyrins Phthalocyanines* **2001**, *5*, 267; d) P. K. Panda, Y. J. Kang, C. H. Lee, *Angew. Chem. Int. Ed.* **2005**, *44*, 4053; *Angew. Chem.* **2005**, *117*, 4121; e) D. Wu, A. B. Descalzo, F. Emmerling, Z. Shen, X. Z. You, *Angew. Chem. Int. Ed.* **2008**, *47*, 193; *Angew. Chem.* **2008**, *120*, 199; f) Y. Chang, H. Chen, Z. Zhou, Y. Zhang, C. Schutt, R. Herges, Z. Shen, *Angew. Chem. Int. Ed.* **2012**, *51*, 12801; *Angew. Chem.* **2012**, *124*, 12973; g) H. Mori, T. Tanaka, A. Osuka, *J. Mater. Chem. C* **2013**, *1*, 2500.

[5] a) A. Mallick, H. Rath, *Chem. Asian. J.*, **2016**, *11*, 986 and references therein; b) A. Mallick, J. Oh, D. Kim, H. Rath, *Chem. Eur. J.*, **2016**, *22*, 5504.

[6] L. S. Fuller, B. Iddon, K. M. Smith, *J. Chem. Soc. Perkin Trans. 1* **1997**, 3465.

[7] J. i. Setsune, Y. Katakami, N. Lizuna, *J. Am. Chem. Soc.* **1999**, *121*, 8957.

[8] a) V. G. Anand, S. k. Pushpan, S. Venkataraman, A. Dey, T. K. Chandrashekar, B. Joshi, R. Roy, W. Teng, K. R. Senge, *J. Am. Chem. Soc.* **2001**, *123*, 8620; b) S. J. Narayanan, B. Sridevi, T. K. Chandrashekar, A. Vij, R. Roy, *Angew. Chem. Int. Ed.* **1998**, *37*, 3394; *Angew. Chem.* **1998**, *110*, 3582; c) S. J. Narayanan, B. Sridevi, T. K. Chandrashekar, A. Vij, R. Roy, *J. Am. Chem. Soc.* **1999**, *121*, 9053; d) S. Shimizu, R. Taniguchi, A. Osuka, *Angew. Chem. Int. Ed.* **2005**, *44*, 2225; *Angew. Chem.* **2005**, *117*, 2265.

[9] M. Gouterman, *J. Mol. Spectrosc.* **1963**, *11*, 108.

[10] a) J.-Y. Shin, K. S. Kim, M.-C. Yoon, J. M. Lim, Z. S. Yoon, A. Osuka, D. Kim, *Chem. Soc. Rev.* **2010**, *39*, 2751; b) J. M. Lim, J.-Y. Yoon, Y. Tanaka, S. Saito, A. Osuka, D. Kim, *J. Am. Chem. Soc.* **2010**, *132*, 3105; c) J. Oh, H. Mori, Y. M. Sung, W. Kim, A. Osuka, D. Kim, *Chem. Sci.* **2016**, *7*, 2239.

[11] J. M. Lim, K. Ganesan, Y. M. Sung, A. Srinivasan, T. K. Chandrashekar, D. Kim, *Chem. Commun.* **2014**, *50*, 4358.

[12] B. Franck, A. A. Nonn, *Angew. Chem. Int. Ed. Engl.* **1995**, *34*, 1795; *Angew. Chem.* **1995**, *107*, 1941.

[13] K. M. Kadish, *Prog. Inorg. Chem.* **1986**, *34*, 435.

[14] a) A. D. Becke, *J. Chem. Phys.* **1993**, *98*, 1372; b) C. Lee, W. Yang, R. G. Parr, *Phys. Rev. B* **1988**, *37*, 785.

[15] CCDC 1025205 contains the supplementary crystallographic data for this paper. These data can be obtained free of charge from The Cambridge Crystallographic Data Centre via www.ccdc.cam.ac.uk/data request/cif.

[16] a) P. v. R. Schleyer, C. Maerker, A. Dransfeld, H. Jiao, N. J. R. v. E. Hommes, *J. Am. Chem. Soc.* **1996**, *118*, 6317.

[17] D. Geuenich, K. Hess, F. Köhler, R. Herges, *Chem. Rev.* **2005**, *105*, 3758.

[18] a) T. M. Krygowski, *J. Chem. Inf. Comput. Sci.* **1993**, *33*, 70; b) T. M. Krygowski, K. M. Cryański, *Chem. Rev.* **2001**, *101*, 1385.

Received: February 26, 2016
Published online on April 25, 2016